J. Physiol. (1980), **307**, *pp.* 217–242
With 11 *text-figures*
Printed in Great Britain

SODIUM CHANNEL PERMEATION IN SQUID AXONS I: REVERSAL POTENTIAL EXPERIMENTS

T. B. BEGENISICH* AND M. D. CAHALAN†

*From the *Department of Physiology, University of Rochester, Rochester, New York 14642, the †Department of Physiology, University of California at Irvine, California 92717 and the Marine Biological Laboratory, Woods Hole, Massachusetts 02543, U.S.A.*

(*Received 19 June 1979*)

SUMMARY

1. Na channel reversal potentials were studied in perfused voltage clamped squid giant axons. The concentration dependence of ion selectivity was determined with both external and internal changes in Na and ammonium concentrations.

2. A tenfold change in the internal ammonium activity results in a 42 mV shift in the reversal potential, rather than the 56 mV shift expected from the Goldman, Hodgkin, Katz equation for a constant P_{Na}/P_{NH_4} ratio. However, changing $[Na]_o$ tenfold at constant internal $[NH_4]$ gives approximately the expected 56 mV shift. Therefore, the apparent channel selectivity depends upon the internal ammonium concentration but not the external Na concentration.

3. With ammonium outside and Na inside, the calculated permeability ratio is nearly constant, regardless of the permeant ion concentration.

4. Internal Cs ions can alter the Na/K permeability ratio.

5. The results are considered in terms of a three-barrier, two-site ionic permeation model.

INTRODUCTION

Recent experiments on the ionic pathways through nerve and bilayer membranes have demonstrated inadequacies in the usual descriptions of ion permeation employing the concept of independent ionic movement developed by Nernst (1888, 1889) and Planck (1890*a*, *b*). These experiments on the Na channel include ionic currents that tend to saturate as the concentration of permeant ions is raised (Hille, 1975*a*, *b*; Begenisich & Cahalan, 1980), and reversal potentials that do not follow the Goldman (1943)–Hodgkin–Katz (1949) equation (Chandler & Meves, 1965; Cahalan & Begenisich, 1975, 1976; Ebert & Goldman, 1976). In K channels, unidirectional flux measurements yield flux ratios that cannot be described by the Ussing (1949) flux equation, unless the ratio is raised to a power of 2·3 (Hodgkin & Keynes, 1955) or as high as 3 (Begenisich & De Weer, 1979). This is not consistent with independent ion movement. Channels in lipid bilayers formed by the antibiotic gramicidin A also show saturation (Myers & Haydon 1972; Läuger, 1973), concentration-dependent selectivity (Sandblom, Eisenman & Neher, 1977; Eisenman, Sandblom & Neher, 1978), and a flux ratio exponent of 2 (Schagina, Grinfeld & Lev, 1978).

0022-3751/80/1890-0296 $07.50

Our goal in this and the following paper is to present a broad range of data on open sodium channels and to test a relatively simple multi-ion permeation model. This paper concerns the ion selectivity of the Na channel, while the next describes current–voltage properties.

The Nernst–Planck and Goldman–Hodgkin–Katz equations predict a shift of 56 mV (at 10 °C) in the zero-current or reversal potential when only one permeant ion is present on each side of the membrane and its concentration is varied tenfold. This 56 mV shift is a cornerstone of the ionic hypothesis and is routinely used to identify the ion passing through a selective channel. Recently, however, it has been demonstrated that at least certain channels need not follow the 56 mV per decade rule. With K as the sole permeant ionic species inside a perfused squid giant axon, there is about a 40 mV shift in the Na channel reversal potential when internal K is varied tenfold. The channel selectivity ratio, P_{Na}/P_K calculated from the Goldman, Hodgkin, Katz potential equation, decreases from 12·8 to 3·5 when the K activity on the axoplasmic side of the membrane is reduced from 355 to 42 mM. This apparent selectivity change was found not to depend on ionic strength, anion permeability, or membrane potential over the 30 mV range studied (Cahalan & Begenisich, 1976).

Does the apparent change in selectivity occur for all permeant ions on the inside? Is the concentration dependence for selectivity seen only at the inner surface of the membrane, or is it a symmetrical property of the channel? To answer these questions, we studied Na channel reversal potentials under essentially bi-ionic conditions in which sodium was the only permeant ion on one side of the membrane and ammonium was the only permeant ion on the opposite side. We find that internal NH_4 does, but internal Na does not, alter Na channel selectivity. Also, neither external NH_4 nor Na produce this effect. The apparent selectivity change, then, is asymmetric with respect to both ion type and membrane surface. Furthermore, we find that the gating process of Na channels has no observable effect on selectivity, and one ion can alter permeability ratio of two other ions. A preliminary account of these results has appeared (Cahalan & Begenisich, 1977).

METHODS

The experiments were performed at the Marine Biological Laboratory in Woods Hole, Massachusetts, on segments of giant axons from *Loligo pealei*. Axons averaging 450 μm were fine cleaned, internally perfused, and studied under voltage clamp. The details of the perfusion technique and the voltage clamp are the same as described previously (Cahalan & Begenisich, 1976; Begenisich & Lynch, 1974). Membrane potentials, V_m, have been corrected for the liquid junction potential at the interface between the internal voltage measuring pipette filled with 0·56 M-KCl, and the internal perfusion solution. The potential outside the axon was measured using a 3 M-KCl agar bridge. Series resistance compensation of 3 $\Omega.cm^2$ was employed in all of the experiments. The temperature was measured by a thermistor next to the axon and maintained at 10 °C by a thermoelectric device. In seventy-five axons bathed in artificial sea water and initially perfused with a standard internal solution of 400 mM-K with 50 mM-fluoride and 320 mM-glutamate as anions (Yeh & Narahashi, 1977), the resting potential averaged −62·3 mV.

Solutions

In these experiments, our goal was to measure Na channel reversal potentials over a range of Na and ammonium concentrations both inside and outside the axon. Ammonium was chosen rather than K because ammonium is more permeant than K and thus could be studied over a

broader concentration range, and also because we found it easier to maintain the membrane holding potential at −70 mV with high external ammonium than with K. Experiments were done with Na and NH_4 on opposite sides of the membrane as the only measurably permeant ions except for the relatively impermeant Ca ions in the external solution.

TABLE 1. Composition of stock external sea-water solutions. Activity coefficients, γ, are listed for the major cation

	γ	[Na] (mM)	[NH_4] (mM)	[Tris] (mM)	[Ca] (mM)
Na sea water	0·68	450	—	5	50
NH_4 sea water	0·63	—	500	5	50
Tris sea water	—	—	—	480	50

TABLE 2. Composition of stock internal solutions. The solutions were buffered with 2·5 mM-HEPES or 10 mM-Tris. Activity coefficients, γ, are given for the major cation

	γ	Sucrose (mM)	Na (mM)	NH_4 (mM)	TMA (mM)	TEA Br (mM)	F (mM)	Glutamate (mM)
Stock NH_4	0·7	440	—	200	—	40	100	100
Stock Na	0·74	490	200	—	—	20	100	100
Stock TMA	—	490	—	—	200	20	100	100
500 NH_4	0·63	—	—	500	—	50	100	400

TABLE 3. Composition of internal solutions for permeant ion interactions. All numbers are concentrations in mM

	K	Cs	TMA	F	Glutamate	TEA
200 K, 325 TMA	200	—	325	100	425	20
200 K, 325 Cs	200	325	—	100	425	20

Three stock artificial sea-water solutions were prepared with Na, NH_4, or Tris as the dominant cation with 50 mM-$CaCl_2$, pH 7·3–7·4 (20 °C). The composition of the stock external solutions is shown in Table 1. The low Na or low NH_4 outside solutions were then prepared by mixing appropriate amounts of Na or NH_4 stock with Tris sea water. The Na external solutions contained 5, 10, 25, 50, or 100% of the stock Na sea water (450 mM-Na), while the NH_4 solutions contained 12·5, 25, 50, or 100% of stock ammonium sea water (500 mM). The osmolarity of the external solutions was kept between 980 and 1020 m-osmole/kg.

The stock internal solutions shown at the top of Table 2 contained 200 mM-Na, NH_4 or tetramethylammonium (TMA), with fluoride and glutamate as anions. Na solutions containing 5, 10, 25 and 50 mM-Na were prepared by diluting the Na stock solutions with appropriate amounts of TMA stock. Similarly, NH_4 solutions were prepared with 5, 10, 20, 50, 100, and 200 mM-NH_4 and complementary amounts of TMA. In addition to these solutions at constant ionic strength with approximately 200 mM salt, a solution was prepared with 500 mM-NH_4. This solution is also shown in Table 2. Other internal solutions are listed in Table 3. Internal solutions contained either 2·5 mM-HEPES or 10 mM-Tris as buffer, pH 7·1–7·3 (20 °C) and also 20–50 mM-tetraethylammonium (TEA) Br to block current through K channels. The osmolarity was maintained at 1000–1040 m-osmole/kg.

Most experiments were done with a series of external or internal solution changes using one solution as a standard to test for reproducibility by bracketing test solutions with the standard. Usually, two different test solutions and one standard solution were used in an experiment. At least 3 min were allowed for internal solution changes. In addition, the reversal potential was checked during the course of a solution change to ensure completeness of exchange.

Recording and analysis

The membrane current signal was amplified, digitized, and stored on the shift register buffers of a signal averager. The design of the averager is similar to that described by Bezanilla & Armstrong (1977). The linear portion of leakage and capacitative currents was electronically subtracted both by analog circuitry and by using a P, $P/4$ pulse pattern as described by Armstrong & Bezanilla (1974). In this procedure, for every pulse of amplitude P given from the normal holding potential near -70 mV, four pulses of amplitude $P/4$ were given from a potential of -130 mV, well negative of the region of significant Na current. The current during the four $P/4$ pulses was subtracted digitally from the current during the P pulse. This technique results

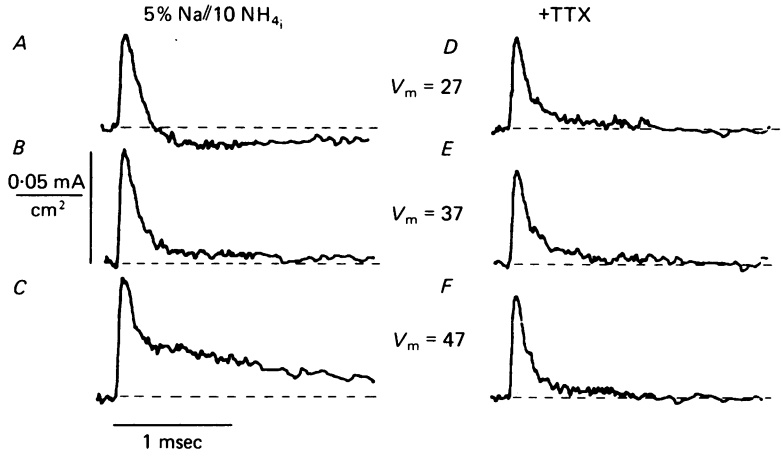

FIG. 1. Membrane currents recorded near V_{rev} with low concentrations of permeant ions. External solution: 5% Na sea water. Internal solution: 10 mM-NH_4, 190 mM-TMA, 20 mM-TEA. In traces D, E and F, 500 nM-tetrodotoxin was added to the external solution. The potential during each depolarizing pulse is indicated between traces.

in good time resolution (10 μsec), and gating currents were normally observed near the Na reversal potential. Sometimes signal averaging was employed with up to five complete pulse cycles to improve the signal-to-noise ratio. The digitized record of current versus time, usually representing one complete $P + 4 \times P/4$ cycle, was stored on a casette tape recorder (Pioneer 2121) using a nine bit digital interface. After the experiment, the traces were read from the tape recorder back into the shift register buffers of the signal averager, and either measured directly from D/A oscilloscope display, or transferred to a PDP 8 computer for further analysis.

Na currents were measured after each solution change over at least a 100 mV range of potentials, with 5 mV intervals near the reversal potential. In general, the currents recorded represent Na currents plus non-linear leakage and capacitance currents. The non-linear portion of leakage current was negligibly small in most experiments compared to the size of the Na currents, but in some experiments with low concentrations of permeant ions 500 nM-tetrodotoxin (TTX) was added externally to provide subtraction of gating currents and non-linear leakage as illustrated in Fig. 1. Traces A, B, and C represent gating and ionic currents near the Na channel reversal potential with 5% Na sea water and 10 mM-internal NH_4. Tetrodotoxin blocks only the ionic current in Na channels leaving the gating current and other possible non-linear ionic currents in traces D, E, and F. Clearly the reversal potential is near 37 mV from a comparison of the left and right traces at the same potentials. Normally, the reversal potential could be estimated by examining where the current trace changed from concave downward to concave upward as the potential step was increased. However, for increased accuracy, peak Na current–voltage plots were made, and a curve was drawn by eye through the points to determine the zero current or reversal potential, V_{rev}, for Na channels. We estimate the precision of the

reversal potential determinations to be within about 2 mV, judging from the reversibility and repeatability of the measurements.

The permeability ratio P_{NH_4}/P_{Na} was computed from the Goldman, Hodgkin, Katz equation for two permeant ions.

(1) $P_{NH_4}/P_{Na} = [Na]_o/[NH_4]_i \exp(-V_{rev}F/RT)$ for Na outside and ammonium inside; or

(2) $P_{NH_4}/P_{Na} = [Na]_i/[NH_4]_o \exp(V_{rev}F/RT)$ for Na inside and ammonium outside. Na and ammonium activities from Robinson & Stokes (1965) rather than concentrations were used in the permeability ratio computations. These activities are given in Tables 4 and 5.

The model

An alternative to the continuum-independence approach is the rate-theory description of ionic permeation (Eyring, Lumry & Woodbury, 1949). Several authors have employed this theory to describe ion permeation phenomena (see review by Hille, 1975*a*). The early theories assumed that no more than one ion could occupy the pore at any one time. Such one-ion models yield voltage-dependent, but not concentration-dependent ionic permeability ratios and flux ratio exponents of unity (Hille, 1975*a*; Hille & Schwarz, 1978, Läuger, 1979; Begenisich & Cahalan, 1979). Therefore, these models can account for saturation, blocking, and some aspects of the selectivity properties of Na channels in nerve (Hille, 1975*b*), but cannot duplicate the unidirectional flux ratio data for K channels or the concentration-dependent selectivity of Na channels and gramicidin channels.

More recent work has focused on multi-ion pores (Hodgkin & Keynes, 1955; Heckmann, 1972; Hladky, 1972; Eisenman, Sandblom & Neher, 1977; Hille & Schwarz, 1978; Begenisich & Cahalan, 1979). One type of multi-ion pore model describes a possible direct replacement of an ion at a site by another ion in a 'knock-on' type of scheme. This type of model predicts concentration-dependent permeability ratios and flux ratio exponents of greater than one, but does not predict the observed saturation of current as the ion concentrations are raised (Begenisich & Cahalan, 1979). We consider here a three-barrier, two-site permeation model that can account for current saturation, current–voltage relations and concentration-dependent selectivity. A detailed description of this model is given in the Appendix.

Fig. 2*A* and *B* show a number of theoretical reversal potential *vs.* ionic concentration relations which simulate our experimental findings and are predicted by the three-barrier, two-site model. For these graphs, the experimental bi-ionic conditions have been duplicated: only ions of type *A* are outside the axon, only ions of type *B* are in the axoplasm. Fig. 2*A* plots the reversal potential as a function of the activity of ion *B* at a fixed *A* activity of 0·15 M. Three curves are shown. For curve 1, the barriers for ion *A* are set at 9, 9, 9 *RT* and for ion *B*, these are 11, 11, 11 *RT*. The wells are all set to zero and the barriers are equally spaced. Curve 2 uses the same parameters as curve 1, except that the innermost *B* barrier is lowered to 10 *RT*. In curve 3, the parameters for ion *A* are as in curves 1 and 2 while the *B* barriers have been changed to 10, 12, 10 *RT*. Fig. 2*B* shows three plots of the reversal potential as a function of external ion *A* activity (ion *B* activity = 0·2 M). The numbers and energy profiles of the curves correspond to those of Fig. 2*A*.

The slope of curve 1 in Fig. 2*A* is about 56 mV per decade. The permeability ratio for the two ions computed from the reversal potentials using the Goldman–Hodgkin–Katz equation would in this case be independent of the ionic concentration. The slopes of curves 2 and 3 in Fig. 2*A* are about 49 mV per decade, resulting in an apparent concentration-dependent permeability ratio. The slopes of all curves in Fig. 2*B* are about 54 mV per decade, or approximately the prediction of the Goldman–Hodgkin–Katz equation. Therefore, changes of external ionic concentration would not, in this case, appear to alter the permeability ratio.

It is clear from Fig. 2 that barrier heights affect not only the absolute value of the reversal potential, but also the slope. Changing the barrier spacing to $2{\cdot}D1 = 2{\cdot}D3 = 0{\cdot}2$, $2{\cdot}D2 = 0{\cdot}6$, produces less than a 2·5 mV change in the reversal potential over the entire range of concentrations shown. Increasing the well depths for ion *A* to -1, -1 *RT* and for ion *B* to -2, -2 *RT* produces less than a 1 mV change in the reversal potential. So reversal potential measurements are rather sensitive tests of barrier heights but do not help in determining the spacing and well depths. In contrast, the data presented in the next paper put constraints on both barrier spacing and (inner) well depth.

Our objective is to describe all the available Na channel permeation data by one set of barriers

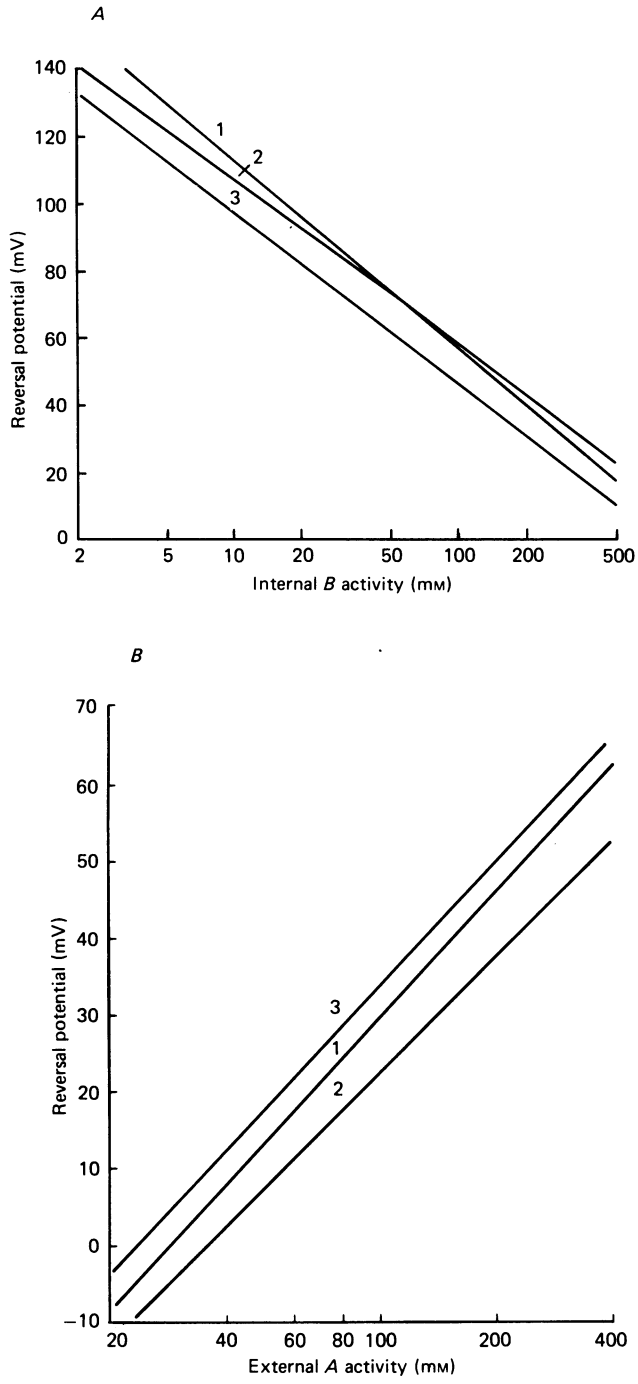

Fig. 2. *A*, reversal potentials at varying ion activities predicted by the three-barrier, two-site model. Reversal potentials were calculated for a membrane with a constant activity of *A* (150 mM) on one side and activities of ion *B* on the other side indicated by the abscissa. Curve 1 energy barriers: ion *A* 9, 9, 9 *RT*; ion *B* 11, 11, 11 *RT*. For curve 2, the innermost *B* barrier was lowered to 10 *RT*. In curve 3 the energy barriers for ion *B* were changed to 10, 12, 10 *RT*. All well depths were set to 0, and the barriers were equally spaced. *B*, calculated reversal potentials for constant *B* activity of 0·2 M and variable activities of ion *A*. The same free energy profiles for the curves in part *A* were used.

and wells for each ion. The procedure for doing this was first to have the computer systematically vary each of the barriers and compare the resulting reversal potentials to the experimental data. After some 15,000 barrier arrangements were examined, the most promising set of barriers was used, and the ionic currents calculated from the model were compared with the current–voltage data in the next paper. The well depths were then determined from the saturation of ionic

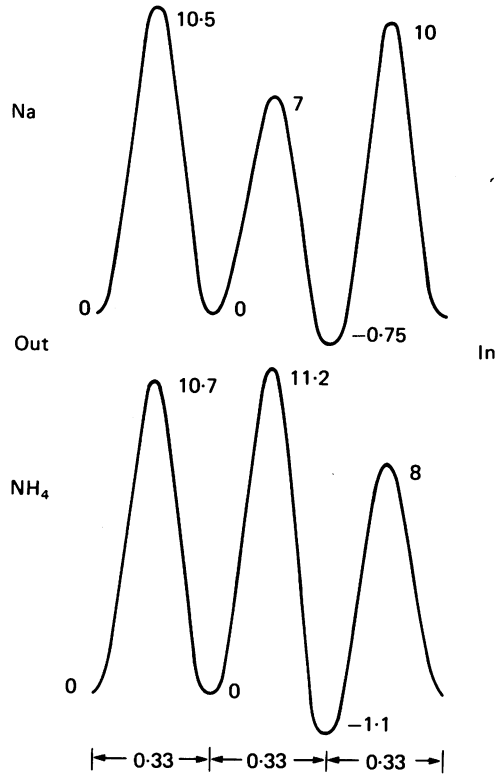

Fig. 3. Free energy profiles for Na and ammonium in the Na channel used in fitting the reversal potential data in this paper and the data in the next paper.

current described in that paper. This process was repeated until one set of model parameters was found that could account for all the experimental observations. These parameters are shown in the energy diagrams for Na and NH_4 illustrated in Fig. 3 and are also given in Table 3 of the next paper. As the calculations above (Fig. 1) and in the following paper illustrate, relatively small changes in the energy profiles would significantly alter the goodness of fit. The final parameters presented here represent a compromise to provide a reasonable fit to all the data.

RESULTS

Experiments with external Na and internal NH_4

Internal ammonium, like K (Cahalan & Begenisich, 1976), alters the Na channel selectivity ratio as calculated from eqn. (1). Fig. 4*A* illustrates voltage clamp currents with three different internal ammonium concentrations spanning a hundred-fold range. The external Na concentration was held constant in this experiment at 50 %

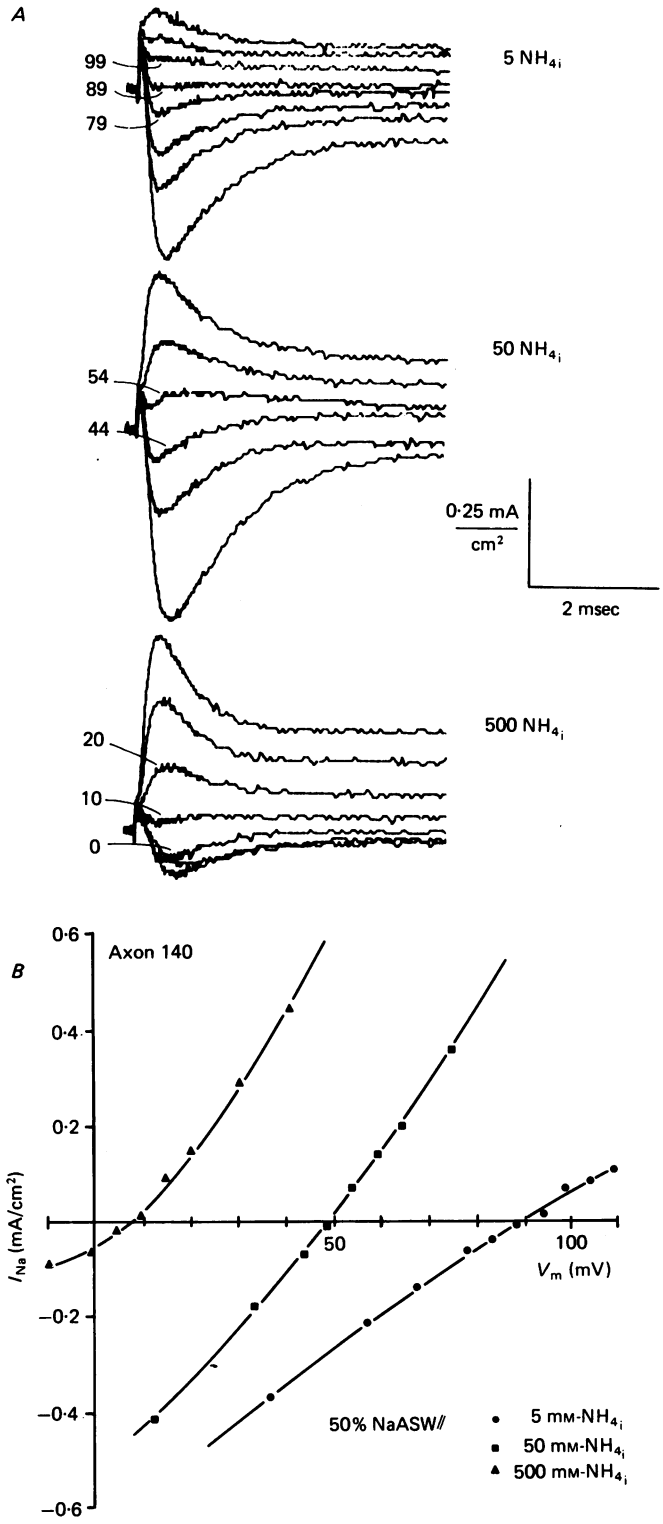

Fig. 4. *A*, currents with 5, 50, and 500 mM-NH_4 inside the axon. The external solution was 50% Na sea water. Membrane potentials for pulses near the reversal potential are indicated by numbers to the left of each voltage clamp family. *B*, TTX-corrected peak Na current–voltage plot for the same experiment as 2*A*.

(225 mM) of the normal artificial sea water. With 5 mM-NH_4, current at 79 mV is surely inward, while at 99 mV current is outward. The reversal potential appears to be near 89 mV. With 50 mM-NH_4 inside the reversal potential drops to between 44 and 54 mV, and with 500 mM-NH_4 the current is zero near 10 mV. Plots of the TTX-corrected peak Na current *vs.* membrane potential for this experiment are illustrated in Fig. 4*B*. The reversal potential shifts from 90 to 49·5 mV to 8 mV on each tenfold increase in internal ammonium. This reversal potential shift of about 41 mV per

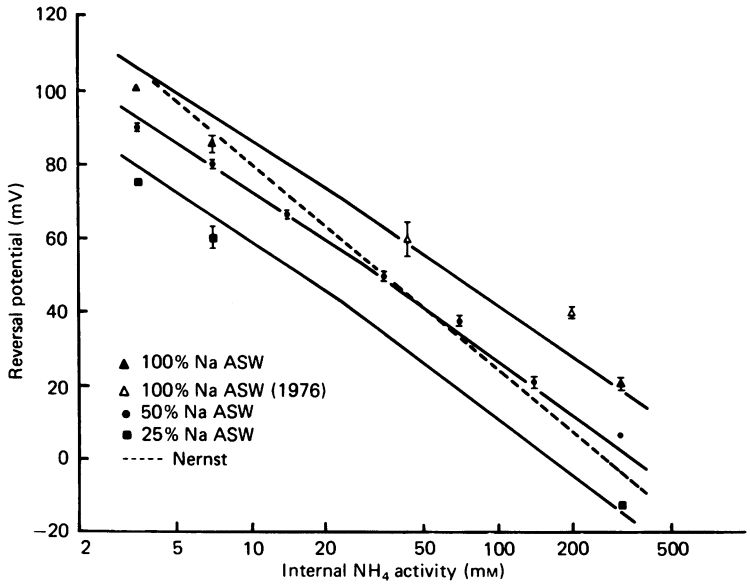

Fig. 5. Relationship between reversal potential and internal ammonium activity. Each set of data points represents a different external sodium concentration. (△) from Cahalan & Begenisich (1976). The dashed line labelled Nernst has a slope of 56 mV per decade. The smooth curves are computed from the two-site model.

tenfold concentration change deviates markedly from the 56 mV shift expected from equation 1 if the selectivity ratio P_{NH_4}/P_{Na} remained constant. Raising the internal ammonium concentration decreases P_{NH_4}/P_{Na}, as calculated from eqn. (1), making the channel appear more selective for Na over ammonium. Specifically, in the experiment of Fig. 4, P_{NH_4}/P_{Na} decreased from 1·07 to 0·56 to 0·35 on each successive tenfold increase in ammonium concentration.

Control experiments reported previously (Cahalan & Begenisich, 1976) demonstrated that the permeability ratio in the Na channel is a function of internal permeant ion activity, rather than ionic strength, TMA concentration, a small degree of anion or Ca permeability, or ion accumulation. In fact, in Fig. 4, the 5 mM and 50 mM-NH_4 internal solutions were at constant ionic strength with TMA as the replacement cation.

In Fig. 5, the results of fourteen experiments are collected to illustrate the relationship between Na channel reversal potential and internal ammonium activity. For a fixed external Na concentration (25, 50, or 100 % of stock Na sea water), the data deviate from the slope of 56 mV per decade shown by the dashed reference line.

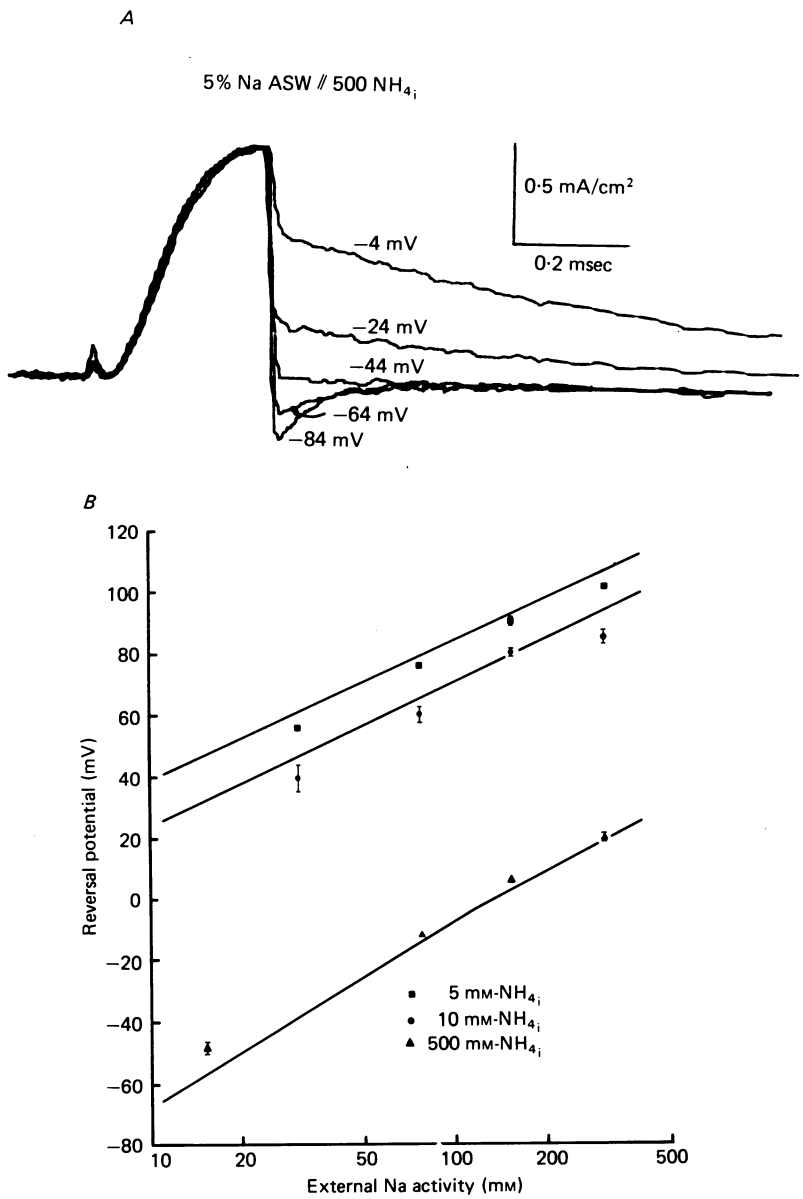

Fig. 6. *A*, Na currents with 5% Na sea water and 500 mM-NH_4 inside. Currents have been TTX corrected by digitally subtracting traces for the same pulse protocol after adding 500 nM-TTX. After a 0·5 msec pulse to 16 mV, the potential was stepped to the potentials indicated on the right of the traces. *B*, relationship between reversal potential and external Na activity. The continuous curves were computed from the two-site model.

Least-squares fits of straight lines (not shown) have been calculated with slopes of about 42 mV per decade NH_4 over a hundred-fold range. This slope indicates an apparent change in channel selectivity with changes in internal ammonium concentration over a large range of external Na concentration. The continuous lines in this Figure are predictions of the three-barrier, two-site model.

In nine experiments, internal NH_4 was held constant while external Na was varied from 100 to 5 % of Na sea water. With 5 % external Na and high concentrations of NH_4 inside, the reversal potential occurred at potentials too negative to produce Na channel activation. In this case, a prepulse was given to open most channels, and instantaneous current–voltage relationships were determined to locate the reversal potential as illustrated in Fig. 6. In this Figure, Na current is first activated by a pulse to 16 mV and then interrupted by pulses to various potentials. The same pulse protocol was repeated after adding 500 nM-TTX to block the Na currents. Subtraction of gating and non-linear leakage currents resulted in the Na current traces shown in Fig. 6*A*. On repolarizing to −44 mV, the current is flat at the base line of zero net current, indicating that this is the reversal potential. Longer duration pulses and different activating prepulses did not change the reversal potential, demonstrating that accumulation of Na ions in the restricted extracellular space (Frankenhaeuser & Hodgkin, 1956) did not occur to an appreciable degree during the brief activating prepulses. With higher external Na concentrations, the reversal potentials were determined from peak current–voltage relations as described previously.

The relation between the reversal potential and external Na activity for three different internal [NH_4] is shown in Fig. 6*B*. A least-squares fit (not shown) to the data points with 500 mM-NH_4 yields a slope of 53·2 mV per decade concentration change, indicating that P_{NH_4}/P_{Na} computed from eqn. (1) did not vary greatly over the twentyfold [Na] activity change, even down to potentials at which the sodium channel gating process is not fully activated. The continuous lines in this Figure are the predictions of the two-site permeation model. The major effect of external Na concentration changes is to produce reversal potentials approximately in accord with eqn. (1) with no change in channel selectivity. Thus, the selectivity change with external Na and internal ammonium is asymmetric: internal NH_4 ions apparently alter selectivity but external Na ions do not.

Table 4 summarizes the results of experiments with external Na and internal ammonium. The reversal potential (mean ± S.E. of mean) and computed permeability ratio P_{NH_4}/P_{Na} (mean ± S.E. of mean) are listed for each solution tested. The permeability ratio tends to remain constant for changes in external Na, whereas an increase in internal ammonium brings about a decrease in the permeability ratio.

Experiments with external NH_4 and internal Na

In order to answer questions concerning the symmetry of the apparent selectivity change, the concentration gradients were reversed, with Na inside and ammonium outside as the permeant ionic species. The procedure for determining reversal potentials was the same as described earlier and a sample experiment is shown in Fig. 7. In this experiment, the axon was internally perfused with 10 mM-Na, 190 mM-TMA, and 20 mM-TEA. With Na inside the axon, the inactivation gating process was often incomplete (Chandler & Meves, 1970). The top set of traces shows currents with

TABLE 4. Reversal potentials and permeability ratios with external Na and internal ammonium. Activities rather than concentrations are listed in the table headings. Reversal potentials and permeability ratios computed from equation 1 are listed as mean ± S.E. of mean where n = the number of axons. Often there were two or more reversal potential determinations for each solution within one experiment

	$[Na_o]$ (mM) 15·3		30·6		76·5		153		306	
$[NH_{4i}]$ (mM)	V_{rev} (mM)	P_{NH_4}/P_{Na}	V_{rev} (mV)	P_{NH_4}/P_{Na}	V_{rev} (mV)	P_{NH_4}/P_{Na}	V_{rev} (mV)	P_{NH_4}/P_{Na}	V_{rev} (mV)	P_{NH_4}/P_{Na}
3·5	—	—	55·9	0·874	75·7	0·97	90·1 ± 0·2	1·07 ± 0·01	100·7	1·38
	—	—	n = 1		n = 1		n = 2		n = 1	
7	—	—	39·5 ± 4·4	0·87 ± 0·16	60 ± 2·7	0·94 ± 0·10	80·1 ± 0·6	0·81 ± 0·02	85·3 ± 2·3	1·33 ± 0·1
			n = 2		n = 4		n = 2		n = 5	
14	—	—	—	—	—	—	66·8 ± 0·24	0·71 ± 0·07	—	—
							n = 3			
35	—	—	—	—	—	—	49·8 ± 0·7	0·56 ± 0·02	—	—
							n = 2			
70	—	—	—	—	—	—	37·3 ± 1·4	0·47 ± 0·03	—	—
							n = 2			
140	—	—	—	—	—	—	21·3 ± 2·2	0·46 ± 0·04	—	—
							n = 3			
315	−48·3 ± 2·2	0·38 ± 0·04	—	—	−12·5	0·41	6·2 ± 0·8	0·38 ± 0·01	20·3 ± 0·5	0·42 ± 0·0
	n = 4				n = 1		n = 2		n = 4	

500 mM-NH_4 outside. Currents are just inward at 79 mV and outward at 89 mV. When the concentration of NH_4 was changed to 62·5 mM, the reversal potential shifted to between 27 and 37 mV. The bottom trace shows the current for a depolarization to 37 mV after adding 500 nM-TTX to illustrate that the Na current in the middle set of traces was barely outward at 37 mV. There may be a small amount (10 μA/cm^2) of residual inward current carried by ammonium ions through K channels, but this current and other non-Na currents do not greatly interfere with the reversal potential

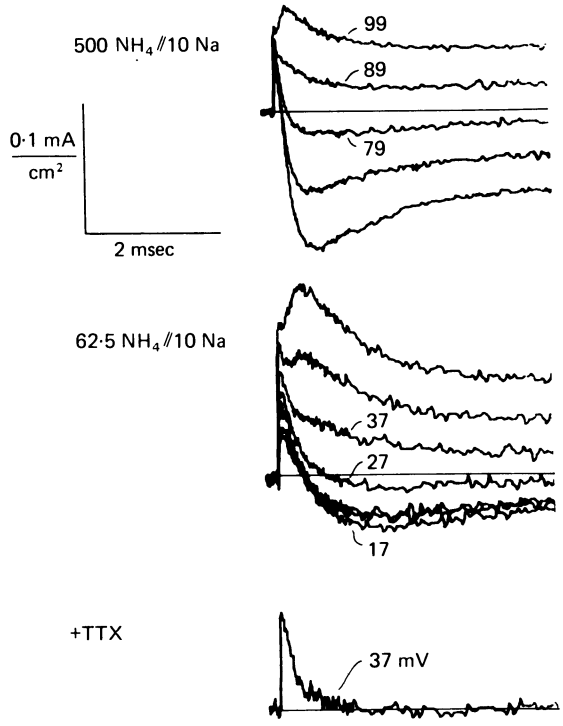

Fig. 7. Currents with ammonium outside and Na inside. The top voltage clamp family represents current with 100% NH_4 sea water outside and 10 mM-Na, 190 mM-TMA inside. The middle set of traces are currents after reducing external NH_4 to 12·5% of the stock NH_4 sea water. The bottom trace is a sample record after adding 500 nM-TTX. Potentials for clamp steps near the reversal potential are indicated.

determination because non-Na currents are small and TTX subtraction was employed. In the experiment of Fig. 7, the reversal potential changed by about 53 mV for the eightfold external NH_4 change. Plots of peak Na channel current–voltage relations were used to determine the reversal potentials with several concentrations of NH_4 outside and 10 mM-Na inside. Data for nine experiments of this type are summarized in Fig. 8. A least-squares fit (not shown) yields a slope of 58·7 mV/decade, slightly greater than that predicted by eqn. (1). The three-barrier, two-site model prediction (continuous lines) is a reasonable representation of the data and does predict a shift of slightly greater than 56 mV. Thus, external ammonium does not appear to alter the selectivity ratio significantly, whereas internal ammonium does.

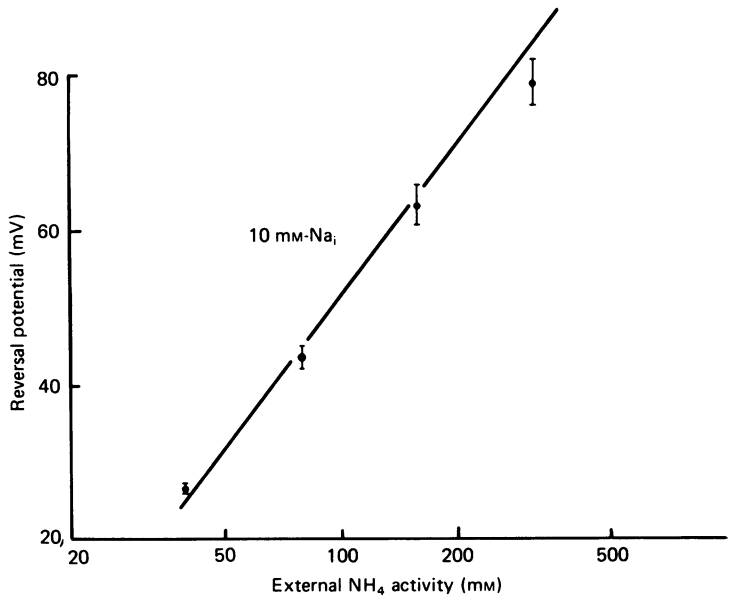

Fig. 8. Relationship between reversal potential and external NH_4 activity. The internal solution is 10 mM-Na, 190 mM-TMA. A least-squares fit (not shown) has a slope of 58·7 mV per decade [NH_4] change. Smooth curve computed from the two-site model.

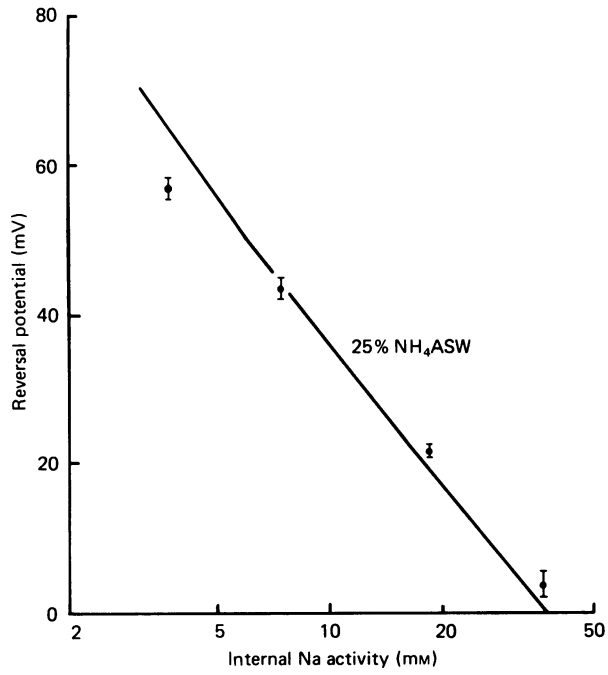

Fig. 9. Reversal potential versus internal Na activity with 25% NH_4 sea water. A least-squares fit (not shown) has a slope of 53·2 mV per decade Na change. Continuous curve computed from the two-site model.

TABLE 5. Reversal potentials and permeability ratios with external ammonium and internal Na. Activities rather than concentrations are listed. Reversal potentials and permeability ratios computed from eq. (2) are listed as mean ± S.E. of mean where n = the number of axons

	$[NH_4]_o$ = 39·4		78·8		157·5		315	
$[Na]_i$	V_{rev} (mV)	P_{NH_4}/P_{Na}	V_{rev} (mV)	P_{NH_4}/P_{Na}	V_{rev} (mV)	P_{NH_4}/P_{Na}	V_{rev} (mV)	P_{NH_4}/P_{Na}
3·7	—	—	56·8 ± 1·5 n = 4	0·49 ± 0·03	—	—	—	—
7·4	26·7 ± 0·5 n = 6	0·56 ± 0·01	43·5 ± 1·4 n = 4	0·57 ± 0·03	63·3 ± 2·7 n = 4	0·65 ± 0·07	79·1 ± 2·9 n = 6	0·63 ± 0·08
18·5	—	—	21·6 ± 1·0 n = 4	0·57 ± 0·02	33·0 n = 1	0·46	—	—
37	—	—	3·9 ± 1·7 n = 3	0·55 ± 0·04	—	—	—	—

If the changes in selectivity are asymmetric with respect to the side of the membrane, as the experiments with internal and external ammonium show, is selectivity also ion-dependent? Internal K, Rb, Cs, ammonium, and guanidinium affect the channel selectivity, while impermeant ions such as TMA or Tris have little or no effect on selectivity (Cahalan & Begenisich, 1976). Fig. 9 illustrates the effect of internal Na concentration on the reversal potential with external NH_4 fixed at 125 mM. The slope of a least-squares fit (not shown) is 53·2 mV per decade concentration change. The solid line shows the prediction from the permeation model. Thus, internal Na has little or no effect on the P_{NH_4}/P_{Na} selectivity ratio.

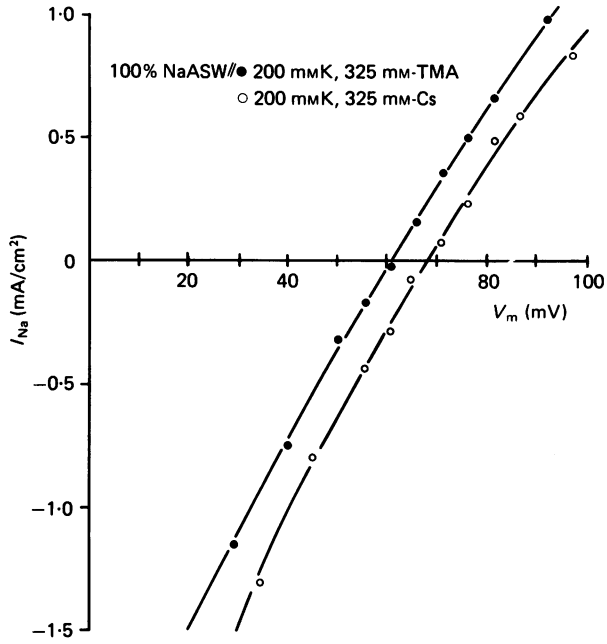

Fig. 10. Current–voltage relations with 200 mM-K inside plus Cs or TMA. The external solution was 100% Na sea water. Curves drawn by eye.

Table 5 summarizes the results with external NH_4 and internal Na. The permeability ratio P_{NH_4}/P_{Na} calculated from eqn. (2) does not vary greatly for either external NH_4 changes or Na changes at either membrane surface.

Modulation of selectivity ratio by a third permeant ion

To see if one permeant ion can affect the selectivity ratio of two others, we introduced Cs into the internal solution with K as the major internal permeant ion, while bathing the axon in Na sea water. Cs is barely permeant through Na channels having a selectivity ratio, P_{Cs}/P_{Na} of about 0·02 at a Cs concentration of 275 mM (Chandler & Meves, 1965; Cahalan & Begenisich, 1976). The effect of Cs was compared with TMA which is not measurably permeant, with a selectivity ratio of less than 0·002. Fig. 10 illustrates current–voltage relationships for an experiment with internal Cs and TMA. The reversal potential is about 61 mV with TMA and 200 mM-K inside. Assuming

no effect of TMA on selectivity, the calculated reversal potential P_K/P_{Na} is 0·17. Because Cs has a measurable permeability in the channel, one would expect a shift in the reversal potential of nearly −4 mV when 325 mM-Cs is substituted for TMA from the following equation for three permeant ions, using $P_{Cs}/P_{Na} = 0{\cdot}02$:

$$V_{rev} = \frac{RT}{F} \ln\{P_{Na}[Na_o]/(P_K[K_i] + P_{Cs}[Cs_i])\}. \quad (3)$$

In fact, the reversal potential shifts in the opposite direction to about 68·5 mV when internal Cs is added in the experiment of Fig. 10.

TABLE 6. Effect of Cs on P_K/P_{Na}. Reversal potentials are mean ± S.E. of mean. The external solution was 100% Na sea water. P_K/P_{Na} was computed from the Goldman, Hodgkin, Katz equation assuming $P_{Cs} = 0$, P_K/P^*_{Na} was recomputed from eqn. (3) assuming $P_{Cs}/P_{Na} = 0{\cdot}02$

Internal solution	V_{rev} (mV)	P_K/P_{Na}	P_K/P^*_{Na}
200 K, 325 TMA	63·5 ± 2·0	0·16 ± 0·01	—
200 K, 325 Cs	71·4 ± 2·8	0·11 ± 0·01	0·075

Table 6 illustrates the effect of Cs on reversal potentials and selectivity ratios for two experiments with four determinations in both solutions. The reversal potential increases by an average of nearly 8 mV on substituting Cs for TMA. The selectivity ratio, P_K/P_{Na}, ignoring Cs permeability decreases from 0·16 to 0·11 when Cs is added. Using eqn. (3) to correct for Cs permeability, the selectivity ratio P_K/P_{Na} decreases from 0·16 to 0·075 when Cs is added.

DISCUSSION

Concentration-dependent selectivity

Mathematical treatments of ion permation based on independent ion movement such as the Goldman, Hodgkin, Katz equation, have been fundamental in describing membrane permeability. However, as described in the Introduction, there are several observations in a variety of ionic channels that indicate the presence of ionic interactions. This is not surprising, since it might be expected at the microscopic level of ions passing through individual channels that the assumption of independent movement of ions in the channel will not be obeyed.

Models employing an Eyring rate theory approach express some of these deviations from the independence principle, most notably saturation of current at high concentrations of permeant ions (Läuger, 1973; Hille, 1975*b*). Because of mathematical simplicity, the models have usually been restricted to the case in which only a single ion at a time can occupy the channel. Though successfully describing many permeability properties, the one-ion pore models cannot account for flux coupling found in K channels (Hodgkin & Keynes, 1955; Begenisich & De Weer, 1977, 1979) or for the concentration-dependent effects on ion selectivity found in Na channels, particularly the asymmetric nature of the concentration dependence (Begenisich & Cahalan, 1979).

Our experiments on sodium channel selectivity demonstrate that permeability

ratios computed from measured reversal potentials using the Goldman–Hodgkin–Katz equation (eqns. (1) and (2)) depend on the concentration of many permeant ions in the axoplasm. Concentration-dependent selectivity is expressed in plots of reversal potential versus activity having slopes less than 56 mV per decade activity change. Lowering the internal activity of K, ammonium, Rb, Cs, and guanidinium apparently decreases the selectivity of the channel for external Na over the internal permeant ions (Cahalan & Begenisich, 1976). Ammonium, at low internal concentrations, for example, becomes as permeant as Na. Impermeant ions like TMA or Tris have no detectable effect on the selectivity ratios, showing that variable selectivity is not produced by changes in internal ionic strength. Na ions, though very permeant, also have little effect on selectivity ratios, either outside or inside the axon. At least one permeant ion (Cs) can alter the selectivity ratio of two others (K and Na). Finally, changes in P_{NH_4}/P_{Na} are asymmetric with respect to the membrane surface, as neither external Na nor ammonium alters the selectivity ratio, while internal ammonium has a strong effect on the selectivity ratio.

Potential dependence and gating

Our results indicate that the membrane potential itself does not result in a change in the selectivity properties of open channels that might occur if some structural or conformational change in the open channel were induced by the membrane field. With decreasing external Na or ammonium, the reversal potential falls smoothly with a slope near 56 mV per decade concentration change over a range of potentials from -50 to $+80$ mV. Hironaka & Narahashi (1977) have measured the resting squid axon membrane permeability to sodium and other externally applied cations at -70 mV, and suggest that their results might be explained by a voltage-dependent Na channel selectivity mechanism. Our results make this interpretation unlikely. The discrepancy might be a result of their measurement of total membrane permeability rather than TTX sensitive, Na channel permeability.

We have observed no detectable effect of the Na channel activation and inactivation gating mechanisms on selectivity ratios. If a single channel could assume multiple states of conductance, one might expect that the different conducting states would have different selectivity properties. Our results are consistent with the notion that channels have only one conducting state or that all conducting states have the same selectivity. At a constant internal concentration of NH_4, P_{NH_4}/P_{Na} remains approximately the same between -50 and 20 mV; this range includes potentials where channels are only partially activated and partially inactivated.

Also, we observed no change in the reversal potential determined from instantaneous current–voltage relations at various times during the activation and inactivation of Na permeability. Single channel conductances, determined from conductance fluctuation measurements in frog node, are independent of the membrane potential both for K channels (Begenisich & Stevens, 1975) and for Na channels (Sigworth, 1977). Both the fluctuation studies and our results on selectivity suggest that most of the Na channel conductance can be attributed to a single conducting state of the channel.

The model

The continuous lines in Figs. 5, 6, 8 and 9 show that a three-barrier, two-site model can reasonably well describe the Na channel reversal potentials over a ten to hundred-fold alteration in external and internal Na and NH_4 activity. The next paper in this series extends the observations to include currents through Na channels as a function of activity and membrane potential.

For ionic pores to show high ionic selectivity, they must have rather small diameters, probably too small for ions to pass in their completely hydrated form. The main obstacle to ionic permeation, then, is likely to be the energy required to remove some water from the ion so it can pass through the pore. These energies are enormous: the standard free energy of transferring Na^+ from a vacuum to an aqueous solution is about -98 kcal/mole (Conway, 1970) or about 160 *RT*. This energy represents complete dehydration; partial dehydration during the passage through the pore is more likely. Even so, in order to obtain low Q_{10}s and high transit rates, the energy difference of an ion between bulk solution and the pore must be kept small, e.g. by substitution of pore carbonyl oxygens for water oxygens (see Mullins, 1959; Hille, 1975*b*).

A second impediment to ionic movement is a barrier called the image potential (Parsegian, 1975). An ion in a finite medium of low dielectric constant induces a charge at the interface of a higher dielectric constant medium and hence is attracted to the interface. Therefore, near the edges of the membrane, the ion is at a lower potential energy than in the middle.

The three-barrier, two-site model embodies these various considerations in a rather simple form. The empirically determined energy profile for NH_4 and K, (see following paper) show a high central barrier and minima of energy toward the edges. The situation is reversed for Na ions: the central barrier is flanked by two larger barriers. It may be the ability of the chemical constituents of the pore to reduce the large 'image' barrier that produces a Na specific pathway. Indeed, Hille & Schwarz (1978) have shown that the conductance of a pore is maximized if there is a low central and large lateral barriers and minimized with a large central barrier. It seems, then, that the empirical barrier diagrams obtained correspond to a system designed to pass Na ions selectively at a high rate.

Hille & Schwarz (1978, following the work of Heckman, 1965 and Hladky, 1972) calculate for the three-barrier model the ionic permeability ratio as defined by the Goldman, Hodgkin, Katz equation. For a low concentration range with very few sites occupied by ions, the permeability ratio depends on voltage and all barrier heights. At intermediate concentrations, the well depths also contribute to this ratio, while at very high concentrations with increasingly complete occupancy of sites, the permeability ratio depends only on the central barriers and on voltage. In our model with 50 % Na sea water, the percentage of channels with no ions goes from 87 % for 5 mM-NH_{4_i} to 46 % for 500 mM-NH_{4_i}, corresponding to a low to intermediate concentration range over which P_{NH_4}/P_{Na} varies more than twofold. In contrast, as external NH_4 is raised from 50 to 300 mM, the percentage of empty channels ranges only from 91 to 76 %, and the permeability ratio is nearly constant. The experimental range of internal Na is too small to appreciably change the degree of occupancy of the

channel. However, with 500 mM-NH_{4_i} changing external Na from 20 to 440 mM decreases the percentage of empty channels from 74 to 37 % and yet the P_{NH4}/P_{Na} ratio is approximately constant over this range of external Na. Thus, changes in channel occupancy alone do not account for the apparent concentration dependence. A definitive answer to the relative contribution of voltage, barrier heights, and well depths to reversal potentials requires an analytical solution to the model.

While the relative barrier heights and well depths were determined as described in the Methods, the absolute values were chosen to produce a Q_{10} for Na current of about 1·4. This is within the 1·3–1·5 range of experimental observations on axons (Hodgkin, Huxley & Katz, 1952; Frankenhaeuser & Moore, 1963; Schauf, 1973).

Once all the barriers and wells have been set, the conductance of a single Na pore can be calculated. However, such a calculation requires a value for the frequency factor as discussed in the Appendix. With external and internal Na activities approximating those of intact axons in sea water (300 mM-Na_o, 50 mM-Na_i), single channel slope conductances at 0 mV of 3 and 50 pmho are computed with the two values of the frequency factor given in the Appendix. These are within an order of magnitude of the value of about 8 phmo for the Na channels of myelinated nerve (Sigworth, 1977; Conti, Hille, Neumcke, Nonner & Stämpfli, 1976) obtained using noise analysis and the values of 4–8 phmo for giant axons obtained from TTX binding studies (see Armstrong, 1975).

Conclusion

The observations on Na channel reversal potentials described here demonstrate that the factors controlling ionic permeation are asymmetric both with regard to ion type and membrane surface. The three-barrier, two-site model accounts qualitatively for these data with asymmetric barriers and wells. In addition, the model predicts several other, as yet untested, properties of the Na channel (see Begenisich & Cahalan, 1980). While the model in its present form can describe ionic permeation in Na channels, some of the fine structure of the model (well spacing, well depths) may eventually need to be altered, as the data on open channel properties become more complete. Perhaps more barriers and wells may ultimately be needed, but the general concepts presented here (inner and outer wells, high central barriers for NH_4 and K, and a low central barrier for Na) will probably remain.

APPENDIX

This Appendix describes both the permeation model used in this and the following report, and the method by which ionic currents and reversal potentials were calculated. The model is a general case of models considered by Chizmadjev, Khodorov & Aityan (1974) and Chizmadjev & Aityan (1977). It is the same as one used by Hille & Schwarz (1978) but the matrix method described here for obtaining solutions is faster than the graph theory technique used by Hille & Schwarz (1978) (see also Heckmann, Vollmerhaus, Kutschera & Vollmerhaus, 1969; Hill, 1966; Lam & Priest, 1972).

We consider here that the channel through the membrane has two local free energy minima (sites) that can either be empty or can contain an ion. Ions move from one site to an adjacent empty site over an intervening energy maximum (barrier). Both sites may be filled simultaneously.

Simple electrostatic calculations show that the coulombic repulsion of two monovalent cations 2 Å apart in a medium of dielectric constant $\epsilon = 20$ is equivalent to about 15 *RT*. If these same ions are 10 Å apart, this energy is reduced to 3 *RT*. The presence of a fixed negative charge in the channel reduces the latter value to a fraction of an *RT* due to the shorter range ion–dipole interactions. These simple calculations are consistent with the more complete calculations of Levitt (1978).

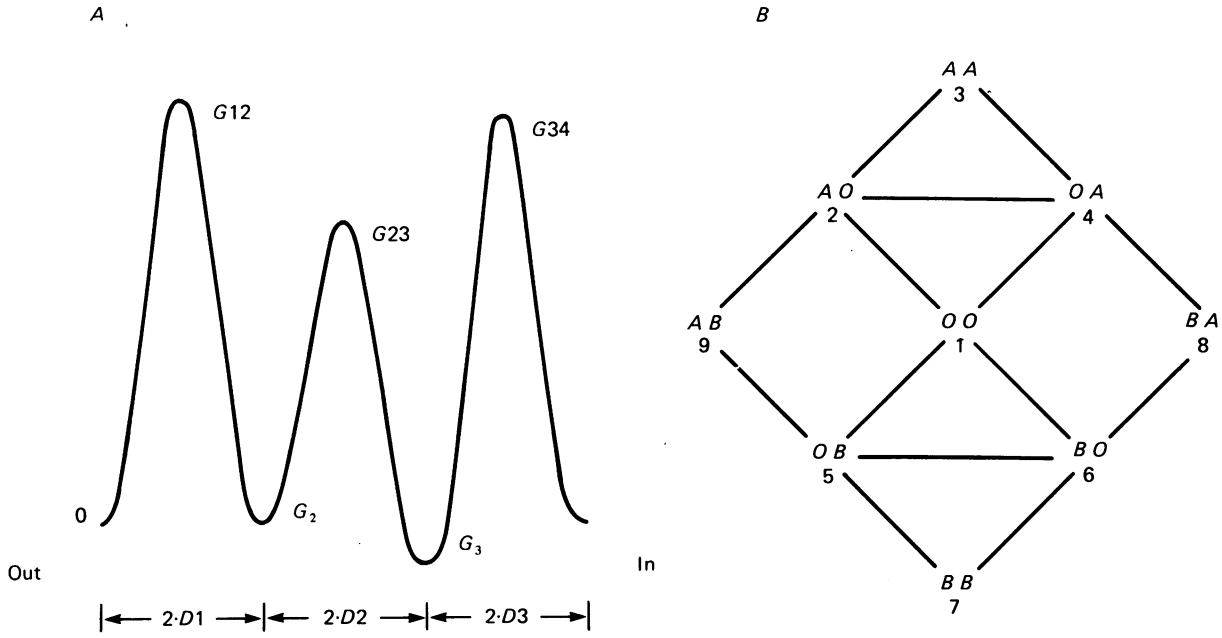

Fig. 11. *A*, arbitrary free energy profile of an ion in the two-site channel. The *G*s are the Gibbs free energies (at zero membrane potential), and the *D*s are the 'electrical distances'. *B*, state diagram showing states of occupancy of two-site channels and the allowed transitions. The empty state (00) can be filled either by ions of type *A* or type *B* or both. The state *AB*, for example, represents occupancy of the outermost site by ion *A* and the inntermost site by ion *B*.

It is reasonable, then, to assume that ions can move only to empty sites and yet allow both sites to be simultaneously occupied. Unlike Hille & Schwarz (1978), we do not include explicit ionic repulsion between ions in this model for three reasons. First, it was not necessary to include such interactions to be able to reproduce most of the experimental data. In fact, preliminary calculations showed that the fits were less satisfactory with repulsion included. Also, the presence of a fixed negative charge in the Na channel of nerve (Hille, 1975) would reduce this interaction. Lastly, inclusion of this interaction would add another adjustable parameter to a model which is already sufficiently complicated.

While most of our experiments were done with bi-ionic conditions, in the model we allow two types of ions (e.g. Na and NH_4) to be on both sides of the membrane. A general energy profile for one type of ion in the model channel is shown in Fig. 11. The nomenclature follows that of Hille (1975*b*). This Figure shows the zero voltage

or 'chemical' part of the free energy of the ions. The electrostatic contribution from the membrane voltage must be added as described later.

With two sites and two types of ions, there are nine possible states for the channel. A diagram of these states and the allowed transition between them is given in Fig. 11 *B*. '0' denotes an empty site which can be filled by an ion of type *A* or *B*. Each state in the diagram is labelled by a small number. Forward, k_{ij}, and reverse, k_{ji}, rate constants connect states i and j. The objective is to determine the probability, P_i, of finding this system in any i^{th} state.

The rate equations written in general form for this system are given by

$$\begin{aligned}
\frac{dP_1(t)}{dt} &= -P_1(t)\sum_{j\neq 1}^{9} k_{1j} + \sum_{j\neq 1}^{9} k_{j1}P_j(t),\\
&\vdots\\
\frac{dP_i(t)}{dt} &= -P_i(t)\sum_{j\neq i}^{9} k_{ij} + \sum_{j\neq i}^{9} k_{ji}P_j(t),\\
&\vdots\\
\frac{dP_9(t)}{dt} &= -P_9(t)\sum_{j\neq 9}^{9} k_{9j} + \sum_{j\neq 9}^{9} k_{j9}P_j(t).
\end{aligned} \tag{A 1}$$

Of the 144 possible rate constants connecting nine states only twenty-eight (fourteen forward and fourteen reverse) are non-zero – these are the allowed transitions shown in Fig. 11*B*. Not all of these rate constants are independent; the free parameters in the model (for fixed barrier spacing) are three barrier heights and two well depths for each ion.

We are interested in the steady-state solution to equations (A 1). In this case, each time derivative term is set equal to zero and eqs. (A 1) become

$$\begin{aligned}
-P_1\sum_{j\neq 1}^{9} k_{1j} + \sum_{j\neq 1}^{9} k_{j1}P_j &= 0,\\
&\vdots\\
-P_i\sum_{j\neq i}^{9} k_{ij} + \sum_{j\neq i}^{9} k_{ji}P_j &= 0,\\
&\vdots\\
-P_9\sum_{j\neq 9}^{9} k_{9j} + \sum_{j\neq 9}^{9} k_{j9}P_j &= 0..
\end{aligned} \tag{A 2}$$

Subject to the conservation equation:

$$\sum_{i=1}^{9} P_i = 1.$$

Equations (A 2) can be written in matrix form:

$$KP = 0$$

$$\text{where } P = \begin{pmatrix} P_1 \\ P_2 \\ \vdots \\ P_9 \end{pmatrix} \text{ and } K = \begin{pmatrix} -\sum_{j\neq 1}^{9} k_{1j} & k_{21} \cdots & k_{91} \\ k_{12} & -\sum_{j\neq 2}^{9} k_{2j} \cdots & k_{92} \\ \vdots & \vdots & \vdots \\ k_{19} & k_{29} \cdots & -\sum_{j\neq 9}^{9} k_{9j} \end{pmatrix}. \tag{A 3}$$

Since $KP = 0$, the matrix K is singular. We found it convenient for computation purposes to make use of the conservation equation to produce a non-homogeneous equation and a non-singular matrix. This was accomplished by dropping the 9th equation in (A 2) and substituting the conservation equation. Then we have

$$DP = R$$

$$\text{where } D = \begin{pmatrix} -\sum_{j\neq 1}^{9} k_{1j} & k_{21} \cdots & k_{81} & k_{91} \\ \vdots & & \vdots & \vdots \\ k_{18} & k_{28} \cdots & -\sum_{j\neq 8}^{9} k_{8j} & k_{98} \\ 1 & 1 & \cdots 1 & 1 \end{pmatrix} \text{ and } R = \begin{pmatrix} 0 \\ 0 \\ \vdots \\ 0 \\ 1 \end{pmatrix}. \tag{A 4}$$

Once the rate constants are determined, eqs. (A 4) can be solved for the Ps using Gauss elimination techniques.

The rate constants are obtained using the principles of absolute reaction rate theory (Glasstone *et al.* 1941). For example, the rate constant for a transition from state 2 to state 4 (which is the rate of ionic movement from well G2 to well G3 over energy barrier G23; see Fig. 11) is given by

$$k_{24} = \nu \exp(-G23 + G2 - D2 \cdot V_m).$$

The first two terms in the exponential represent the intrinsic (non-voltage dependent) part of the free energies (divided by RT). The last term is the contribution the membrane potential, V_m, makes to the free energy. ν is a frequency factor in sec^{-1}. The value of ν in the usual Eyring formulations is kT/h (k is Boltzmann's constant and h is Planck's constant) which is approximately $5{\cdot}8 \times 10^{12}$ sec^{-1} at 10 °C. Recently Hill (1975) has argued that for reactions in solution this factor should be replaced by $D/R\Lambda$, where D is the ionic diffusion constant, R the 'capture distance', and Λ the deBroglie wavelength of the reacting species. For Na ions, $D = 1{\cdot}5 \times 10^{-5}$ cm^2/sec and with $R = 2{\cdot}3$ Å, the value of ν becomes 3×10^{11} sec^{-1}. Only relative currents need be calculated for determining reversal potentials so an exact value of ν is not necessary to be able to use this model. Where necessary (e.g. in k_{12})the rate constants include the ionic concentrations.

After the rate constants and steady-state probabilities are obtained, the steady-state flux for each ion can be calculated as the net rate of ions crossing any one barrier. It is convenient to choose the middle barrier for this, and the fluxes of ions A and B are

$$\begin{aligned} F_A &= P_4 \cdot k_{42} - P_2 \cdot k_{24} \\ F_B &= P_5 \cdot k_{56} - P_6 \cdot K_{65}. \end{aligned} \tag{A 5}$$

The numerical calculation for this model were performed on a Data General Corp. Nova 3 computer. The computation of the net current at one membrane voltage level takes about 1 sec. Reversal potentials were obtained using a Newton–Raphson technique which usually requires only a few iterations to converge. A typical reversal potential calculation takes about 5 sec.

We are indebted to Dr Clay M. Armstrong for providing laboratory space and encouragement at the Marine Biological Laboratory, Woods Hole, Massachusetts. Financial support was provided

by grants nos. NS14609, NS-14138, NS00322 (RCDA) from the National Institutes of Health and by the Muscular Dystrophy Association.

REFERENCES

ARMSTRONG, C. M. (1975). Ionic pores, gates, and galing currents. *Q. Rev. Biophys.* **7**, 179–210.

ARMSTRONG, C. M. & BEZANILLA, F. (1974) Charge movement associated with the opening and closing of the activation gates of the Na channels. *J. gen. Physiol.* **63**, 533–552.

BEGENISICH, T. & CAHALAN, M. (1979). Non-independence and selectivity in sodium channels, in press. *Membrane Transport Processes, vol. 3: Ion Permeation through Membrane Channels*, ed. STEVENS, C. F. & TSIEN, R. W. New York: Raven.

BEGENISICH, T. & CAHALAN, M. (1980). Sodium channel permeation in squid axons II: Non-independence and current–voltage relations. *J. Physiol.* **307**, 243–257.

BEGENISICH, T. & DE WEER, P. (1977). Ionic interactions in the potassium channel of squid giant axons. *Nature, Lond.* **269**, 710–711.

BEGENISICH, T. & DE WEER, P. (1979). Evidence that the K channel of squid axons is a multiple ion pore. *Biophys. J.* **25**, 192*a*.

BEGENISICH, T. & LYNCH, C. (1975). Effects of internal divalent cations on voltage clamped squid axons. *J. gen. Physiol.* **63**, 675–689.

BEGENISICH, T. & STEVENS, C. F. (1975). How many conductance states do potassium channels have? *Biophys. J.* **15**, 843–846.

BEZANILLA, F. & ARMSTRONG, C. M. (1977). A low cost signal averager and data acquisition device. *Am. J. Physiol.* **232**, *C*211–215.

CAHALAN, M. & BEGENISICH, T. (1975). Internal K^+ alters sodium channel selectivity. *Biophys. J.* (*Abstr.*) **15**, 261*a*.

CAHALAN, M. & BEGENISICH, T. (1976). Sodium channel selectivity: dependence on internal permeant ion concentration. *J. gen. Physiol.* **68**, 111–125.

CAHALAN, M. & BEGENISICH, T. (1977). Asymmetric ionic concentration dependence of sodium channel selectivity. *Biophys. J* .**17**, 13*a*.

CHANDLER, W. K. & MEVES, H. (1965). Voltage clamp experiments on internally perfused giant axons. *J. Physiol.* **180**, 788–820.

CHANDLER, W. K. & MEVES, H. (1970). Slow changes in membrane permeability and long lasting action potentials in axons perfused with fluoride solutions. *J. Physiol.* **211**, 707–728.

CHIZMADJEV, Y. A. & AITYAN, S. K. (1977). Ion transport across sodium channels in biological membranes. *J. theor. Biol.* **64**, 429.

CHIZMADJEV, Y. A., KHODOROV, B. I. & AITYAN, S. K. (1974). Analysis of the independence principle for the sodium channels of biological membranes. *Bioelectrochem. Bioenergetics* **1**, 301–312.

CONTI, F., HILLE, B., NEUMCKE, B., NONNER, W. & STÄMPFLI, R. (1976). Measurement of the conductance of the sodium channel from current fluctuations at the node of Ranvier. *J. Physiol.* **262**, 699–727.

CONWAY, B. E. (1970). Some aspects of the thermodynamic and transport behavior electrolytes. In *Physical Chemistry: An Advanced Treatise IXA*, ed. EYRING, H., chap. 1, pp. 1–166. New York: Academic.

EBERT, G. & GOLDMAN, L. (1976). The permeability of the sodium channel in *Myxicola* to the alkali cations. *J. gen. Physiol.* **68**, 327–340.

EISENMAN, G., SANDBLOM, J. & NEHER, E. (1977). Ionic selectivity, saturation, binding and block in the gramicidin A channel: A preliminary report. In *Metal–Ligand Interactions in Organic Chemistry and Biochemistry*, part 2, ed. PULLMANN, B. & GOLDBLUM, N. Dordrecht, Holland: D. Reidel Publishing Company.

EISENMAN, G., SANDBLOM, J. & NEHER, E. (1978). Interactions in cation permeation through the gramicidin channel. *Biophys. J.* **22**, 307–340.

EYRING, H., LUMRY, R. & WOODBURY, J. W. (1949). Some applications of modern rate theory to physiological systems. *Record Chem. Progress* **100**, 100–114.

FRANKENHAEUSER, B. & HODGKIN, A. L. (1956). The after effects of impulses in the giant nerve fibres of *Loligo*. *J. Physiol.* **131**, 341–376.

FRANKENHAUSER, B. & MOORE, L. E. (1963). The effect of temperature on the sodium and potas-

sium permeability changes in myelinated nerve fibres of *Xenopus laevis*. *J. Physiol.* **169**, 431–437.

GOLDMAN, D. E. (1943). Potential, impedance, and rectification in membranes. *J. gen. Physiol.* **27**, 37–60.

HECKMANN, K. (1965). Zur Theorie der 'single file' Diffusion., II. *Z. Phys. Chem.* **46**, 1–25.

HECKMANN, K. (1972). Single file diffusion. In *Biomembranes, vol. 3, Passive Permeability of Cell Membranes*, ed. KREUZER, F. & SLEGERS, J. F. G., pp. 127–153. New York: Plenum Press.

HECKMANN, K., VOLLMERHAUS, W., KUTSCHERA, J. & VOLLMERHAUS, E. (1969). Mathematische Modelle fur reaktionskinetische Phanomene. *Z. Naturforschung Teil B Anorg. Chem. Org. Chem. Biochem. biophys. Biol.* **24**, 664–673.

HILL, T. L. (1966). Studies in irreversible thermodynamics. IV. Diagrammatic representation of steady-state fluxes for unimolecular systems. *J. theor. Biol.* **10**, 442–459.

HILL, T. L. (1975). Effect of rotation on the diffusion controlled rate of ligand-protein association. *Proc. natn. Acad. Sci. U.S.A.* **72**, 4918–4922.

HILL, T. L. (1976). Diffusion frequency factors in some simple examples of transition-state rate theory. *Proc. natn. Acad. Sci. U.S.A.* **73**, 679–683.

HILLE, B. (1975*a*). Ionic selectivity of Na and K channels in nerve membranes. In *Membranes – A Series of Advances*, vol. 3, ed. EISENMAN, G., chap. 4. New York: Marcel Dekker, Inc.

HILLE, B. (1975*b*). Ionic selectivity, saturation, and block in sodium channels: A four-barrier model. *J. gen. Physiol.* **66**, 535–560.

HILLE, B. & SCHWARZ, W. (1978). Potassium channels as single file pores. *J. gen. Physiol.* **72**, 409–442.

HIRONAKA, T. & NARAHASHI, T. (1977). Cation permeability ratios of sodium channels in normal and grayanotoxin-treated squid axon membranes. *J. membrane Biol.* **31**, 359–381.

HLADKY, S. B. (1972). The mechanism of ion conduction in thin lipid membranes containing gramacidin A. Ph.D. Thesis, University of Cambridge, Cambridge, England.

HODGKIN, A. L., HUXLEY, A. F. & KATZ, B. (1952). Measurement of current voltage relations in the membrane of the giant axon of *Loligo*. *J. Physiol.* **116**, 424–448.

HODGKIN, A. L. & KATZ, B. (1949). The effect of sodium ions on the electrical activity of the giant axon of the squid. *J. Physiol.* **108**, 37–77.

HODGKIN, A. L. & KEYNES, R. D. (1955). The potassium permeability of a giant nerve fibre. *J. Physiol.* **128**, 61–88.

LÄUGER, P. (1973). Ion transport through pores: a rate theory analysis. *Biochim. biophys. Acta* **311**, 423–441.

LAM, C. F. & PRIEST, D. G. (1972). Systematic generation of valid King–Altman patterns. *Biophys. J.* **12**, 248–256.

LEVITT, D. G. (1978). Electrostatic calculations for an ion channel. I. Energy and potential profiles and interactions between ions. *Biophys. J.* **22**, 209–220.

MOZHAYEVA, G. N., NAUMOV, A. P., NEGULYAEV, Y. A. & NOSYREVA, E. D. (1977). The permeability of aconitine-modified sodium channels to univalent cations in myelinated nerve. *Biochim. biophys. Acta* **466**, 461–473.

MULLINS, L. J. (1959). The penetration of some cations into muscle. *J. gen. Physiol.* **42**, 817.

MYERS, V. B. & HAYDON, D. A. (1972). Ion transfer across lipid membranes in the presence of gramicidin A. II. The ion selectivity. *Biochim. biophys. Acta* **274**, 313–322.

NERNST, W. (1888). Zur Kinetik der in Losung befindlichen Korper: Theorie der Diffusion. *Z. phys. Chem.* **2**, 613–637.

NERNST, W. (1889). Die elektromotorische Wirksamkeit der Ionen. *Z. phys. Chem.* **4**, 129–181.

PARSEGIAN, V. A. (1975). Ion–membrane interactions as structural forces. *Ann. N.Y. Acad. Sci.* **264**, 161–174.

PLANCK, M. (1890*a*). Ueber die Erregung von Elektricitat und Warme in Elektrolyten. *Ann. Physio. u. Chem., Neue folge* **39**, 161–186.

PLANCK, M. (1890*b*). Ueber die Potentialdifferenz zevischen zure verdunnten Losungen binarer Elktrolyte. *Ann. Physik. u. Chem. Neue folge* **40**, 561–576.

ROBINSON, R. A. & STOKES, R. H. (1965). *Electrolyte Solutions*, 2nd edn. London: Butterworth.

SANDBLOM, J., EISENMAN, G. & NEHER, E. (1977). Ionic selectivity, saturation, and block in gramicidin A channels. *J. membrane Biol.* **31**, 383–417.

SCHAGINA, L., GRINFELD, A. E. & LEV, A. A. (1978). Interaction of cation fluxes in gramicidin A channels in lipid bilayer membranes. *Nature, Lond.* **273**, 243–245.

SCHAUF, C. L. (1973). Temperature dependence of the ionic current kinetics of *Myxicola* giant axons. *J. Physiol.* **235**, 197–205.

SIGWORTH, F. (1977). Sodium channels in nerve apparently have two conductance states. *Nature, Lond.* **270**, 265–266.

YEH, J. Z. & NARAHASHI, T. (1977). Kinetic analysis of pancuronium interaction with sodium channels in squid axon membranes. *J. gen. Physiol.* **69**, 293–324.